Jurnal Teknologi

Full paper

Electrodeposited Germanium On Silicon Substrate Using A Mixture Of Germanium Tetrachloride And Propylene Glycol

Mastura Shafinaz Zainal Abidin[a,*], Shahjahan[b], Mohamad Rusop Mahmood[c], Abdul Manaf Hashim[b]

[a]Faculty of Electrical Engineering, Universiti Teknologi Malaysia, 81310 UTM Johor Bahru, Johor Malaysia
[b]Malaysia-Japan International Institute of Technology, Universiti Teknologi Malaysia, Jalan Semarak, Kuala Lumpur 54100, Malaysia
[c]Faculty of Electrical Engineering, Universiti Teknologi MARA, Selangor, Shah Alam 40450, Malaysia

[*]Corresponding author: mastura@fke.utm.my

Article history

Received: 7 July 2014
Received in revised form:
7 October 2014
Accepted: 1 December 2014

Graphical abstract

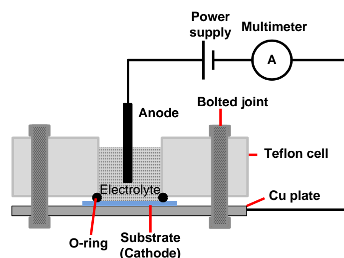

Abstract

We report the deposition of germanium (Ge) film on silicon (Si) substrate by a simple and low cost electrochemical deposition using a mixture of germanium tetrachloride ($GeCl_4$) and propylene glycol ($C_3H_8O_2$). The effects of deposition environment and applied current density on the properties of deposited Ge films were investigated. Ge film containing germanium dioxide (GeO_2) microclusters was obtained for deposition in air-exposed environment while high purity Ge film with no impurity detectable by energy-dispersive x-ray spectroscopy (EDS) was obtained in nitrogen (N_2) filled environment. In Raman spectra, N_2 exposed sample shows smaller full width at half maximum (FWHM) values of Ge-Ge peak compared to air exposed sample, thereby indicating better crystallinity of Ge. Relatively flat and smooth Ge surfaces with the average roughnesses of 0.828-1.069 nm were obtained for all tested current densities of 10, 20 and 60 $mAcm^{-2}$. The mean Ge crystallite grain sizes were determined to be in the range of 2-4 nm. In qualitative voltammetry study, two reduction peaks were observed in cyclic voltammograms measurement which confirms that the deposition of Ge at cathode occurs via two reduction processes. It is expected that the impurity-free Ge film on Si is promising for various device application towards heterogeneous integration on Si platform.

Keywords: Germanium, silicon, current density, electrochemical deposition

© 2012 Penerbit UTM Press. All rights reserved.

1.0 INTRODUCTION

The performance of present silicon ultra-large-scale-integrated-circuits (Si-ULSIs) has been significantly improved by the miniaturization of transistors. [1-4] However, further miniaturization down to nano-scale regime seems to be impractical due to the increase in gate leakage current [5-6], short channel effect [6-7] etc. The most promising breakthrough to further increase the performance of ULSIs is to introduce new channel materials with superb properties such as germanium (Ge) [1,8-15] and compound semiconductors [16-20] on Si platform. Interestingly, these materials are not only being used to increase the performance of conventional complementary metal-oxide-semiconductor (CMOS) transistors, but also to fabricate new transistors with different operating principles such as tunnel field effect transistor (FET) [21], plasma wave device [22-23] etc, as well as to fabricate various kinds of functional devices such as sensors [24-26], optical devices [27], detectors [28-30], solar batteries [31] and ultra-high frequency electronic devices. [32-34] Heteroepitaxial structures of these materials on the Si platform is more beneficial since Si is a cheap material and available in large wafer size. In addition, Si technology is mature and a combination with Si based devices is still needed for certain purposes. Therefore, the growth of high quality materials on Si, particularly Ge films in this present study, is highly required in order to realize such concept of heterogeneous integration.

The typical technique to grow high quality epitaxial Ge films directly on Si is chemical vapour deposition (CVD) [35-37] and molecular beam epitaxy (MBE). [38-40] However, these techniques require precise control of growth parameters and are very costly. Other techniques such as sputtering and evaporation commonly produce amorphous or polycrystalline layer [41-42] and more contaminated Ge/Si interface, which could prevent the crystallization by the subsequent processes such as rapid melting process. [42-43] As an alternative of these techniques, we employed a simple and low cost electrochemical deposition to deposit Ge film on Si substrates in this work.

In electrochemical deposition technique, electrolytes or medium solvents play an important role in the quality of deposited materials. An electrochemical deposition of semiconductor material has been mainly achieved in non-aqueous solvents [44] such as a mixture ionic liquids and glycols. [45-49] For example, the first attempt for electrodeposition of Ge from a solution of germanium tetrachloride ($GeCl_4$) in

propylene glycol ($C_3H_8O_2$) was made by Szekely. [48; 49] A thick Ge layer was successfully formed on metal substrates such as copper and nickel substrates at certain range of temperatures. Saitou *et al.* also had successfully fabricated crystalline Ge thin films on copper substrates using a mixture of $GeCl_4$ and $C_3H_8O_2$ at room temperature. [50] Those works have mostly shown that Ge was successfully electrodeposited on metal substrates. However, metal substrates used might limit the power and the potential of the process. More researches about electrodeposition on semiconductor substrates seems better to understand the capability of electrodeposition technology that offers more established applications related to semiconductor devices. Eventhough Freyland et al. already reported that Ge could be deposited on hydrogenated silicon, H-Si (111) about a decade ago [51], a different electrolyte mixture was attempted in this present paper. In this work, Ge was electrodeposited from a mixture of $GeCl_4$ and $C_3H_8O_2$ while $[BMIM]^+PF_6^-$ saturated with $GeCl_4$ mixture was employed in Freyland et al.'s work. [51] With that, it was proven that the mixture of $GeCl_4$ and $C_3H_8O_2$ is an alternative electrolyte available for Ge electrodeposition. Besides that, further investigations on the effects of deposition environment and applied current density on the properties of electrodeposited Ge on Si also were studied in this paper.

■2.0 EXPERIMENTAL

An n-type phosphorus-doped Si (100) wafer with thickness of 355-405 µm and resistivity of 0.7-1.3 Ωcm was used. The as-received $GeCl_4$ (Merck) and $C_3H_8O_2$ (Merck) were used without any purification treatment. A non-aqueous electrolyte formed by 5% $GeCl_4$ in $C_3H_8O_2$ was used. The electrochemical deposition process was carried out at room temperature in a simple teflon cell by using two terminal configuration where Si substrate which is the piece to be deposited, acts as a cathode and platinum (Pt) wire acts as an anode. Since Pt is an inert anode, it is expected there will be no impurities reaction will take place and affect on the quality of resulted deposited Ge. The schematic of the experimental setup is illustrated in Figure 1.

The effect of deposition environment was investigated by performing the electrodeposition in open air (denoted as sample A) and nitrogen (N_2) (denoted as sample B). In this case, the deposition was done at constant current density, J of 20 $mAcm^{-2}$ for 30 min and other deposition parameters such as electrolyte type, anode and cathode were kept same for both samples. Next, the effect of applied current density on Ge electrodeposition was investigated by applying J of 10 $mAcm^{-2}$ (sample C), 20 $mAcm^{-2}$ (sample D) and 60 $mAcm^{-2}$ (sample E) with 60 min deposition time. For these experiments, all processes including the electrolyte preparation and deposition were done in a N_2 purged glove box.

Prior to deposition process, all samples were cleaned by standard RCA process and diluted hydrofluoric (HF) acid to remove native oxide layer. After deposition, the samples were rinsed with deionized water. The structural, compositional and morphological properties of the deposited Ge on Si substrate were characterized using Raman spectroscopy (Horiba Jobin Yvon: Ar^+ laser, 514 nm wavelength, 20 mW power), field-emission scanning electron microscopy equipped with energy-dispersive x-ray spectroscopy (FESEM-EDS, Hitachi SU8030), and atomic force microscopy (AFM, XE-100 Park).

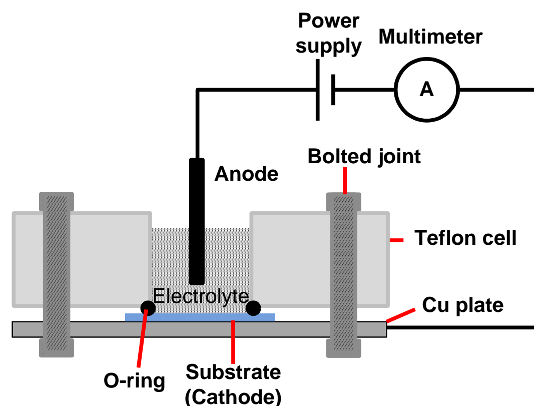

Figure 1 Schematic of electrochemical deposition setup.

■3.0 RESULTS AND DISCUSSION

i. Effect of deposition environment:

Samples denoted as sample A and B are used to evaluate the effect of deposition environment on the properties of deposited film. Physically, smooth silver-like bright color films were obtained for both samples. Figure 2(a) and (b) show the surface morphologies captured by FESEM and EDS spectra for sample A and B, respectively. The deposited layers seem to show flat and smooth surface but some microclusters seem to appear on sample A. The EDS spectra confirm the presence of small amount of oxygen (O) element besides Ge element in sample A. On other hand, there is no O or other impurity element detectable with EDS in the sample B. We speculate that the observed cluster-like structures are formed due to the effect of O element since we observed that germanium dioxide (GeO_2) tend to form cluster-like structures as reported in ref. [52-53] The measured Raman spectrum is used to clarify GeO_2 structure.

Figure 3 shows the measured Raman spectra of both sample A and B. No strong peak at 520 cm^{-1} which corresponds to the Si phonon mode, indicating that the deposited Ge was considerably thick. The penetration of 514 nm Ar^+ laser seems to be limited to 20 nm depth in Ge. [54] The significant Ge-Ge vibrational mode peak (near to 300 cm^{-1}) was observed in both sample A and B [55], indicating that Ge was deposited in both ambient condition. However, this Ge-Ge peak for sample A was slightly broader with a value of full width half maximum (FWHM) of 38.83 cm^{-1} compared to sample B with FWHM of 14.02 cm^{-1}. These values of both samples are relatively large compared to crystalline Ge (c-Ge) which is 3.2 cm^{-1} . [56] This may due to the dominant amorphous structure. This was also proven by appearance of shoulder peak within 210-280 cm^{-1} range that associated to amorphous-Ge (a-Ge). [57] It was not shown here that we also confirm the structure to be amorphous by using electron back scattering diffraction (EBSD). In addition, appearance of another small significant peak corresponds to GeO_2 (164 cm^{-1}) was also observed in sample A. Therefore, we assume that the observed clusters on sample A likely to be GeO_2. We speculate that Ge deposited in open air environment tends to form GeO_2 structure together with Ge layer. It suggests that the process in air-free ambient is needed in order to achieve electrodeposited Ge layer without any impurity.

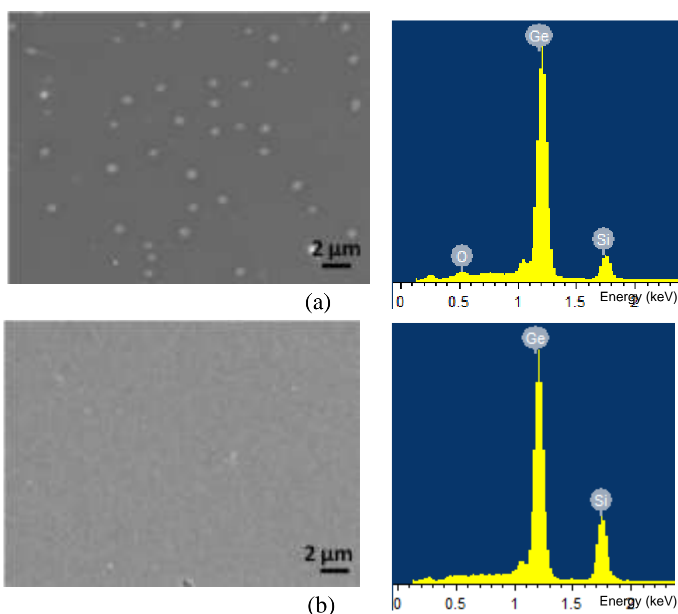

Figure 2 FESEM images and EDS spectra of Ge deposited on Si in (a) open air (Sample A) and (b) N_2 (Sample B) environment.

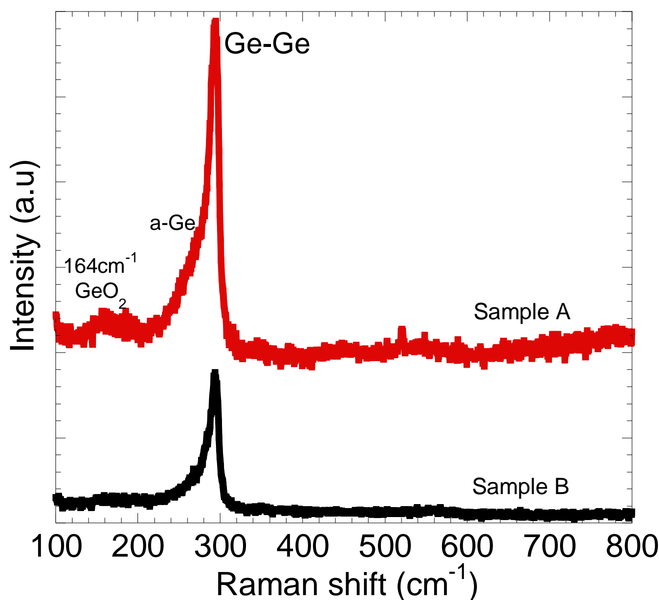

Figure 3 Raman spectra of Ge deposited on Si substrate in open-air (sample A) and N_2 (sample B) ambient.

From this result, it can be assumed that a hydrolysis of $GeCl_4$ and glycol solution in open-air environment leads to the formation of GeO_2. Due to the hygroscopic nature, we assume that glycol solutions have absorbed moisture from the atmosphere during deposition process. As a result, humidity from the air seems to contribute oxygen for the reaction with $GeCl_4$, thereby, leading to the formation of GeO_2 microclusters before being deposited on Si substrate. The possible chemical reaction in the solution is proposed as follows:

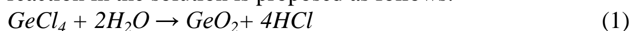

$$GeCl_4 + 2H_2O \rightarrow GeO_2 + 4HCl \quad (1)$$

These GeO_2 microclusters then will be deposited together with Ge layer on Si substrate.

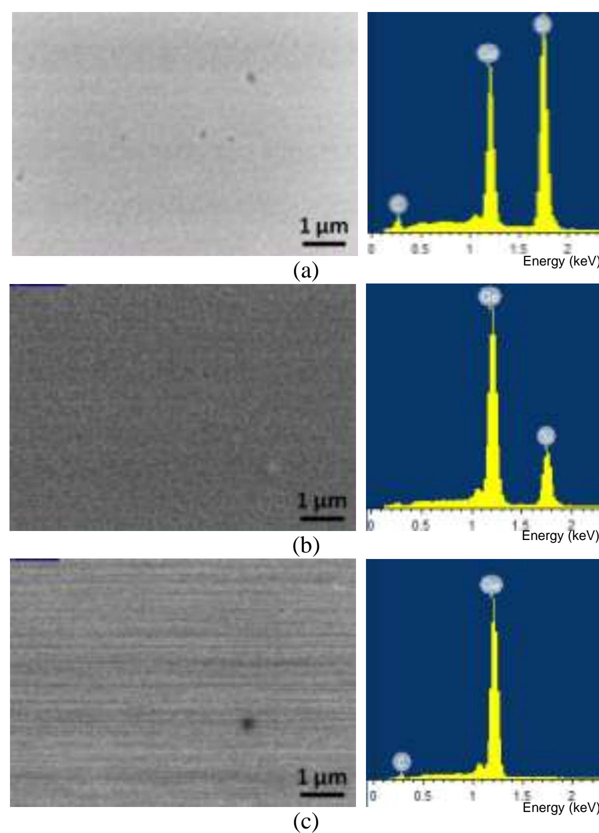

Figure 4 FESEM images and EDS spectra of Ge deposited on Si at current of (a) 10 $mAcm^{-2}$ (Sample C), (b) 20 $mAcm^{-2}$ (Sample D), and (c) 60 $mAcm^{-2}$ (Sample E).

ii. Effect of current density:

Based on the result described in previous section, for the investigation on the effect of current density, all processes including the electrolyte preparation and deposition were done in a N_2 purged glove box in order to reduce the air effect on electrolyte as well as on substrate. The current densities of 10, 20 and 60 $mAcm^{-2}$ were applied to samples denoted as sample C, D and E, respectively.

Figure 4(a)-(c) show the surface morphologies and EDS spectra for sample deposited at J of 10, 20 and 60 $mAcm^{-2}$, respectively. It can be seen that the deposited layers seem to show flat and smooth surface. It is noted that a small atomic ratio of carbon (C) element could be due to C background signal contributed by hydrocarbon contamination from the chamber surfaces, vacuum pumps and sample surface. This C peak usually fast grows when the beam is positioned in the spot mode. [58]

Further observation using AFM had confirmed the uniform and relatively smooth Ge films were electrodeposited on Si substrate. The two-dimensional (2D) and three-dimensional (3D) AFM images of all three samples were shown in Figure 5. The roughness in root-mean-square (RMS) was estimated to be 0.964, 0.828 and 1.069 nm for sample C, D and E, respectively. These roughness values are relatively small and show no significant change among the samples.

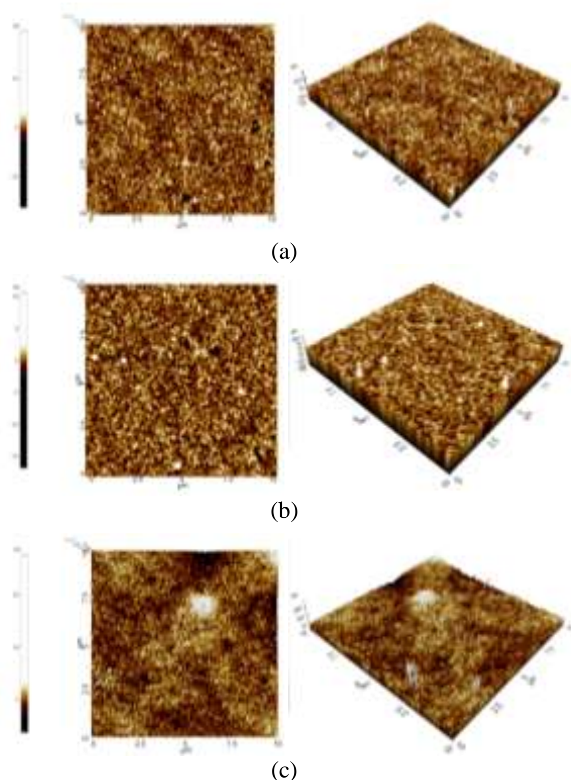

Figure 5 Two-dimensional (2D) and three-dimensional (3D) AFM images (10 µm x 10 µm) of Ge deposited on Si (a) Sample C, (b) Sample D, and (c) Sample E.

The Raman spectra of samples C, D, and E measured at room temperature are shown in Figure 6. The strong Ge-Ge peak near 300 cm^{-1} indicates the deposition of pure Ge on all samples. [55] The FWHM values for respective samples are 8.63 cm^{-1}, 10.79 cm^{-1} and 11.79 cm^{-1}. These values are still wider than that of single c-Ge (3.2 cm^{-1}). [56] Therefore, it suggests that the as-deposited Ge layer is amorphous. It is worth to note here that the crystallization of electrodeposited a-Ge can be achieved by subsequent annealing process known as rapid melting process. [59-61] There is no peak at 520 cm^{-1} which corresponds to the Si phonon. This may be caused by considerably thick Ge layer that deposited on Si substrates. As measured by surface profiler, the thicknesses of deposited Ge for these samples are in the range of 100 to 200 nm. No evidence of Si-Ge alloy mode was observed near 400 cm^{-1} region indicating that intermixing of Si and Ge from Ge/Si interfaces was not aggressive or not happened. It has been reported that the intermixing of Ge-Si could be formed by further annealing process. [56, 62]

The mean Ge grain size can be estimated based on peak shift as compared to that of the bulk c-Ge (at 300 cm^{-1}). The mean Ge crystallite grain size d (in nm) can be calculated from the following equation [63-64]:

$$d = 2\pi\left(\frac{B}{\Delta\omega}\right)^{\frac{1}{2}} \quad (2)$$

where $\Delta\omega$ is the peak shift for the microcrystalline as compared to that of the bulk c-Ge (at 300 cm^{-1}) and $B = 0.96$ nm^2cm^{-1} for Ge. [63-64] The average Ge nanocrystallite size was estimated to be around 3.77 nm, 3.00 nm and 3.02 nm due to peak shift of 2.67 cm^{-1}, 4.23 cm^{-1}, and 4.13 cm^{-1}, respectively. It can be noticed that no significant change in crystallize size for all tested current densities.

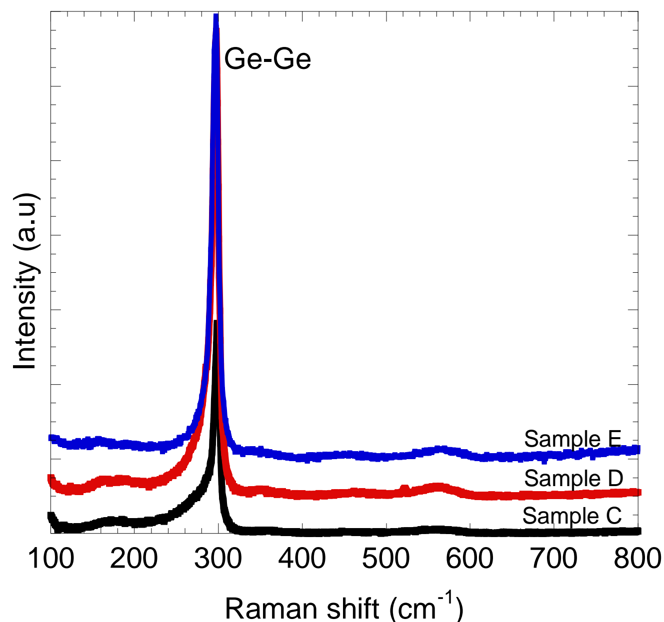

Figure 6 Measured Raman spectra at room temperature for sample C, D and E.

iii. Electrochemical deposition mechanism:

The cyclic voltammograms have been performed in order to generally understand the qualitative study of Ge electrochemical deposition process. This analysis comprises of studying current-potential (I-U) curve to briefly understand the different electrochemical reactions that take place at the substrate interface.

Figure 7 shows the voltammogram of $GeCl_4$:$C_3H_8O_2$ electrolyte done at a sweep rate of 10 $mVsec^{-1}$. On the passage of electricity, germanium will get oxidized (forward scan) before reduction process (backward scan) takes place as reported by Martineau *et al.* [65] The first reduction peak at 0.25 V can be correlated to the reduction of Ge (IV) to Ge (II) while the second peak at -1.5 V corresponds to deposition of Ge. From these results, it can be confirmed that the electrochemical deposition of Ge at cathode (Si substrate) actually occurs via two reduction processes.

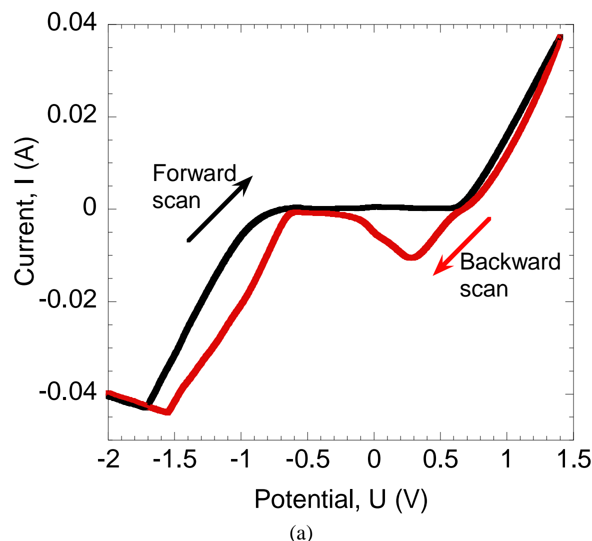

(a)

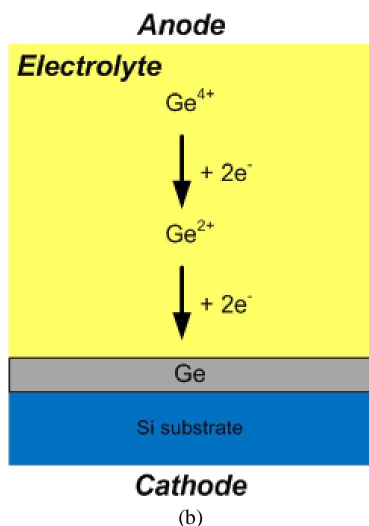

(b)

Figure 7 (a) Typical voltammogram of $GeCl_4$:$C_3H_8O_2$ electrolyte with a scan rate of 10 mVs^{-1} at 25°C. (b) Schematic representation of Ge electrodeposition mechanism.

■4.0 CONCLUSION

In this study, we demonstrated that the proposed electrochemical method can be used to deposit high purity Ge film on Si substrate without any impurity. However, it requires that all processes including the electrolyte preparation and deposition to be done in air-free or recommended to be fully N_2 environment, so that the air effect on electrolyte as well as substrates can be eliminated and the formation of GeO_2 microclusters can be avoided. The deposited Ge layers show amorphous structure with smooth and flat surface. Two reduction peaks were observed in cyclic voltammograms measurement which confirms that the deposition of Ge at cathode occurs via two reduction processes. It is expected that the impurity-free of Ge film on Si is promising for various device application towards heterogeneous integration on Si platform.

Acknowledgement

M. S. Z. A. thanks Universiti Teknologi Malaysia (UTM) and the Ministry of Higher Education Malaysia (MOHE) for the financial supports during her internship at Kyushu University, Japan. The authors wish to extend their thanks for the measurement facilities provided by the Department of Electronics, Kyushu University. This work is partly sponsored by NSG grant from Nippon Sheet Glass Corp., RU grant and MJIIT grant from UTM, FRGS grant and ERGS grant from MOHE.

References

[1] Thompson, S.E., and S. Parthasarathy. 2006. Moore's law: the future of Si microelectronics. *Mater. Today*. 20 – 25.

[2] Murphy, B.T., D.E. Haggan, and W.W. Troutman. 2000. From circuit miniaturization to the scalable IC. *Proc. IEEE*. 88: 691–703.

[3] Theis, T.N. 2003. Beyond the silicon transistor: personal observations. *Comput. Sci. Eng*. 5: 25–29.

[4] Chau, R., M. Doczy, B. Doyle, S. Datta, G. Dewey, J. Kavalieros, B. Jin, M. Metz, A. Majumdar, and M. Radosavljevic. 2004. Advanced CMOS transistors in the nanotechnology era for high-performance, low-power logic applications. *Proceedings of 7th International Conference on Solid-State and Integrated Circuits Technology*. 21: 26–30.

[5] Gehring, A., and S. Selberherr. 2004. Gate leakage models for device simulation. *Proceedings of 7th International Conference on Solid-State and Integrated Circuits Technology*. 972: 971–976.

[6] Timp, G., K.K. Bourdelle, J.E. Bower, F.H. Baumann, T. Boone, R. Cirelli, K. Evans-Lutterodt, J. Garno, A. Ghetti, H. Gossmann, M. Green, D. Jacobson, Y. Kim, R. Kleiman, F. Klemens, A. Kornlit, C. Lochstampfor, W. Mansfield, S. Moccio, D.A. Muller, I.E. Ocola, M.I. O'Malley, J. Rosamilia, J. Sapjeta, P. Silverman, T. Sorsch, D.M. Tennant, W. Timp, and B.E. Weir. 1998. Progress toward 10 nm CMOS devices. *Technical Digest in International Electron Devices Meeting*. IEDM. 615–618.

[7] Ng, K.K., S.A. Eshraghi, and T.D. Stanik. 1993. An improved generalized guide for MOSFET scaling. *IEEE Trans. Electron Devices*. 40: 1895–1897.

[8] Wistey, M., U. Singisetti, G. Burek, E. Kim, B.J. Thibeault, A. Nelson, J. Cagnon, Y.-J. Lee, S.R. Bank, S. Stemmer, P.C. McIntyre, A.C. Gossard, and M.J. Rodwell. 2009. III-V/Ge Channel Engineering for Future CMOS. *ECS Trans.* 19: 361–372.

[9] Takagi, S., M. Sugiyama, T. Yasuda, and M. Takenaka. 2009. Ge/III-V Channel Engineering for Future CMOS. *ECS Trans.* 19: 9–20.

[10] Nayfeh, A., C. Chi On, T. Yonehara, and K.C. Saraswat. 2005. Fabrication of high-quality p-MOSFET in Ge grown heteroepitaxially on Si. *IEEE Electron Device Lett.* 26: 311–313.

[11] Zhiyuan, C., J.-S. Park, J. Bai, L. Jizhong, J. Hydrick, J. Fiorenza, and A. Lochtefeld. 2008. Aspect ratio trapping heteroepitaxy for integration of germanium and compound semiconductors on silicon. *9th International Conference on Solid-State and Integrated-Circuit Technology*. ICSICT 2008. 1425–1428.

[12] Ahmed, A.H.Z., and R.N. Tait. 2005. Characterization of an amorphous GexSi1-xOy microbolometer for thermal imaging applications. *IEEE Trans. Electron Devices*. 52: 1900–1906.

[13] Jawad, M.J., M.R. Hashim, and N.K. Ali. 2010. Hydrogen sensor based on Schottky barriers of Pd/GeO_2 using a low cost electrochemically deposited thin GeO_2 film. *2010 International Conference on Enabling Science and Nanotechnology (ESciNano)*. 1–2.

[14] Khan, M.A., M. Farhan, and T.P. Hogan. 2009. Low temperature synthesis of germanium oxide nanowires by thermal evaporation of germanium in an oxidizing environment. *Nanotechnology Materials and Devices Conference*. NMDC '09. IEEE. 5–8.

[15] Wang, K.L., C. Dongho, L. Jianlin, and C. Chen. 2007. Ge/Si Self-Assembled Quantum Dots and Their Optoelectronic Device Applications. *Proc. IEEE*. 95: 1866–1883.

[16] Gao, Q., J.H. Kang, H.H. Tan, H.E. Jackson, L.M. Smith, J.M. Yarrison-Rice, J. Zou, and C. Jagadish. 2011. Growth and characterization of compound semiconductor nanowires on Si. *11th IEEE Conference on Nanotechnology* (IEEE-NANO). 44–47.

[17] Cantoro, M., C. Merckling, S. Jiang, W. Guo, N. Waldron, H. Bender, A. Moussa, B. Douhard, W. Vandervorst, M.M. Heyns, J. Dekoster, R. Loo, and M. Caymax. 2012. Towards the Monolithic Integration of III-V Compound Semiconductors on Si: Selective Area Growth in High Aspect Ratio Structures vs. Strain Relaxed Buffer-Mediated Epitaxy. *Compound Semiconductor Integrated Circuit Symposium (CSICS)*. IEEE. 1–4.

[18] Datta, S., and R. Chau. 2005. Silicon and III-V nanoelectronics. *International Conference on Indium Phosphide and Related Materials*. 7–8.

[19] Hill, R.J.W., A. Baraskar, C. Park, J. Barnett, P. Majhi, and R. Jammy. 2010. Compound semiconductors on silicon for future generation VLSI. *2010 IEEE International SOI Conference* (SOI). 1–3.

[20] Caymax, M., C. Merckling, W. Gang, T. Orzali, G. Weiming, W. Vandervorst, J. Dekoster, N. Waldron, and A. Thean. 2012. Epitaxy of III-V based channels on Si and transistor integration for 12-10nm node CMOS. *2012 International Conference on Indium Phosphide and Related Materials* (IPRM). 159–162.

[21] Boucart, K., and A.M. Ionescu. 2007. Double-Gate Tunnel FET With High-k Gate Dielectric. *IEEE Trans. Electron Devices*, 54: 1725–1733.

[22] Veksler, D.B., A.V. Muraviev, T.A. Elkhatib, K.N. Salama, and M.S. Shur. 2007. Plasma wave FET for sub-wavelength THz imaging. *2007 International Semiconductor Device Research Symposium*. 1–2.

[23] Hashim, A.M., S. Kasai, and H. Hasegawa. 2008. Observation of first and third harmonic responses in two-dimensional AlGaAs/GaAs HEMT devices due to plasma wave interaction. *Superlattices Microstruct*. 44: 754–760.

[24] Liu, Y., K. Gopalafishan, P.B. Griffin, K. Ma, M.D. Deal, and J.D. Plummer. 2004. MOSFETs and high-speed photodetectors on Ge-on-insulator substrates fabricated using rapid melt growth. *IEDM*

Technical Digest. IEEE International Electron Devices Meeting. 1001–1004.
[25] Abidin, M.S.Z., A.M. Hashim, M.E. Sharifabad, S.F.A. Rahman, and T. Sadoh. 2011. Open-Gated pH Sensor Fabricated on an Undoped-AlGaN/GaN HEMT Structure. *Sensors*. 11: 3067–3077.
[26] Mazuina, M., M. Fong Yee, and H. Abdul Manaf. 2008. The Sensing Performance of Undoped-AlGaN/GaN/Sapphire HEMT Hydrogen Gas Sensor. *Asia International Conference on Modelling & Simulation*. 985–986.
[27] Itabashi, S., H. Nishi, T. Tsuchizawa, T. Watanabe, H. Shinojima, S. Park, K. Yamada, Y. Ishikawa, and K. Wada. 2010. Integration of optical devices based on Si, Ge and SiOx. *2010 7th IEEE International Conference on Group IV Photonics* (GFP). 48–50.
[28] Wang, J., and S. Lee. 2011. Ge-Photodetectors for Si-Based Optoelectronic Integration. *Sensors*. 11: 696–718.
[29] Herman, M.A. 1997. Silicon-germanium heterostructures: properties, technology, and application in infrared detectors. *Opto-Electr. Rev.* 5: 191–204.
[30] Michel, J., J. Liu, and L.C. Kimerling. 2010. High-performance Ge-on-Si photodetectors. *Nat. Photonics* 4: 527–534.
[31] Claeys, C., and E. Simoen. 2007. Germanium-Based Technologies: From Materials to Devices. *Elsevier Science*. Amsterdam.
[32] Eastman, L.F. 1983. Summary Abstract: Compound semiconductor structures for high speed, high frequency devices. *J. Vac. Sci. Technol., B*. 1: 455–455.
[33] Trew, R.J., M.W. Shin, V. Gatto. 1996. Wide bandgap semiconductor electronic devices for high frequency applications. *Technical Digest of 18th Annual Gallium Arsenide Integrated Circuit (GaAs IC) Symposium*. 6–9.
[34] Hashim, A.M., F. Mustafa, S.F.A. Rahman, and A.R.A. Rahman. 2011. Dual-Functional On-Chip AlGaAs/GaAs Schottky Diode for RF Power Detection and Low-Power Rectenna Applications. *Sensors*. 11: 8127–8142.
[35] McComber, K.A., L. Jifeng, J. Michel, and L.C. Kimerling. 2009. Low-temperature germanium ultra-high vacuum chemical vapor deposition for back-end photonic integration. *6th IEEE International Conference on Group IV Photonics*. GFP '09. 137–139.
[36] McComber, K.A., X. Duan, J. Liu, J. Michel, and L.C. Kimerling. 2012. Single-Crystal Germanium Growth on Amorphous Silicon. *Adv. Func. Mater*. 22: 1049–1057.
[37] Fujinaga, K. 1991. Low-temperature heteroepitaxy of Ge on Si by GeH4 in gas low pressure chemical vapor deposition. *J. Vac. Sci. Technol., B*. 9: 1511–1516.
[38] Barski, A., M. Derivaz, J.L. Rouviere, and D. Buttard. 2000. Epitaxial growth of germanium dots on Si(001) surface covered by a very thin silicon oxide layer. *Appl. Phys. Lett.* 77: 3541–3543.
[39] Yang, R., K. Li, G. Li, C. Peng, and Y. Li. 2001. The properties of epitaxial pure germanium films on silicon substrate. *Proceedings of 6th International Conference on Solid-State and Integrated-Circuit Technology*. 631: 634–636.
[40] Larrson, M., A. Eflving, M.I. Hussain, P.O. Holtz, and W.-X. Ni. 2004. Luminescence properties of Ge quantum dots produced by MBE at different temperatures. *First IEEE International Conference on Group IV Photonics*. 124–126.
[41] Huang, S., Z. Xia, H. Xiao, J. Zheng, Y. Xie, and G. Xie. 2009. Structure and property of Ge/Si nanomultilayers prepared by magnetron sputtering. *Surf. Coat. Technol*. 204: 558–562.
[42] Huang, Q., S.W. Bedell, K.L. Saenger, M. Copel, H. Deligianni, and L.T. Romankiwa. 2007. Single-Crystalline Germanium Thin Films by Electrodeposition and Solid-Phase Epitaxy. *Electrochem. Solid-State Lett*. 10: D124–D126.
[43] Going, R., L. Tsu-Jae King, and M.C. Wu. 2013. Rapid melt grown germanium gate photoMOSFET on a silicon waveguide. *IEEE Photonics Conference* (IPC). 38–39.
[44] Lokhande, C.D., and S.H. Pawar. 1989. Electrodeposition of Thin Film Semiconductors. *Phys. Status Solidi A*. 111: 17–40.
[45] Endres, F., and S.Z.E. Abedin. 2002. Nanoscale electrodeposition of germanium on Au(111) from an ionic liquid: an in situ STM study of phase formation. *Phys. Chem. Chem. Phys*. 4: 1640–1657.
[46] Endres, F. 2004. Ionic Liquids: Promising Solvents for Electrochemistry. *Z. Phys. Chem*. 218: 255–283.
[47] Mukhopadhyay, I. and W. Freyland. 2003. Thickness induced metal–nonmetal transition in ultrathin electrodeposited Ge films. *Chem. Phys. Lett*. 377: 223–228.
[48] Szekely, G. 1951. Electrodeposition of Germanium. *J. Electrochem. Soc*. 98: 318–324.
[49] Szekely, G. 1951. Electroplating of Germanium. *US Patt.* 2.
[50] Saitou, M., K. Sakae, and W. Oshikawa. 2002. Evaluation of crystalline germanium thin films electrodeposited on copper substrates from propylene glycol electrolyte. *Surf. Coat. Technol*. 162: 101–105.
[51] Freyland, W., C.A. Zell, S.Z.E. Abedin, and F. Endres. 2003. Nanoscale electrodeposition of metals and semiconductors from ionic liquids. *Electrochim. Acta*. 48: 3053–3061.
[52] Yan, W.X., D. Lian, D.G. Fang, W. Peng, W. Wei, W.L. Duo, and Q. Yong. 2009. Synthesis and characterization of nano/microstructured crystalline germanium dioxide with novel morphology. *Chin. Sci. Bull*. Science in China Press. 2810–2813.
[53] Jawad, M.J., M.R. Hashim, and N.K. Ali. 2011. Synthesis, Structural, and Optical Properties of Electrochemically Deposited GeO_2 on Porous Silicon. *Electrochem. Solid-State Lett.* 14: D17–D19.
[54] Strain measurements of a Si cap layer deposited on a SiGe substrate determination of Ge content, *H.J. Yvon*, (Ed.). from http://www.intercovamex.com/biblioteca_de_aplicaciones/SEMICONDUCTORES/Mediciones%20de%20tension%20de%20de%20una%20capa%20de%20Si%20depositada%20en%20un%20sustrato%20de%20SiGe.%20Determinacion%20del%20contenido%20de%20Ge.pdf
[55] Jawad, M.J., M.R. Hashim, N.K. Ali, E.P. C´orcoles, and M.E. Sharifabad. 2012. An Alternative Method to Grow Ge Thin Films on Si by Electrochemical Deposition for Photonic Applications. *J. Electrochem. Soc*. 159: D124–128.
[56] Miyao, M., T. Tanaka, K. Toko, and M. Tanaka. 2009. Giant Ge-on-Insulator Formation by Si–Ge Mixing-Triggered Liquid-Phase Epitaxy. *Appl. Phys. Express*. 2: 045503.
[57] Mestanza, S.N.M., J.W. Swart, I. Doi, and N.C. Frateschi. 2006. Synthesis of Ge Nanocrystals Grown by Ion Implantation and Subsequent Annealing. *Proceedings of the 6th International Caribbean Conference on Devices, Circuits and Systems*. 151–155.
[58] Rolland, P., V. Carlino, and R. Vane. 2004. Improved Carbon Analysis with Evactron Plasma Cleaning. *Microsc. Microanal*. 10: 964–965.
[59] Hashim, A.M., M. Anisuzzaman, S. Muta, T. Sadoh, and M. Miyao. 2012. Epitaxial-template structure utilizing Ge-on-insulator stripe arrays with nano-spacing for advanced heterogeneous integration on Si platform. *Jpn. J. Appl. Phys*. 51: 06FF04.
[60] Toko, K., T. Sakane, T. Tanaka, T. Sadoh, and M. Miyao. 2009. Defect-free single-crystal Ge island arrays on insulator by rapid-melting-growth combined with seed-positioning technique. *Appl. Phys. Lett*. 95: 112107–112103.
[61] Abidin, M.S.Z., R. Matsumura, M. Anisuzzaman, J.-H. Park, S. Muta, M.R. Mahmood, T. Sadoh, and A.M. Hashim. 2013. Crystallization of Electrodeposited Germanium Thin Film on Silicon (100). *Materials*. 6: 5047–5057.
[62] Sadoh, T., K. Toko, M. Kurosawa, T. Tanaka, T. Sakane, Y. Ohta, N. Kawabata, H. Yokoyama, and M. Miyao. 2011. SiGe-Mixing-Triggered Rapid-Melting-Growth of High-Mobility Ge-On-Insulator. *Key Eng. Mater*. 470: 8–13.
[63] Liu, F.Q., Z.G. Wang, G.H. Li, and G.H. Wang. 1998. Photoluminescence from Ge clusters embedded in porous silicon. *J. Appl. Phys*. 83: 3435–3437.
[64] Abd Rahim, A.F., M.R. Hashim, M. Rusop, N.K. Ali, and R. Yusuf. 2012. Room temperature Ge and ZnO embedded inside porous silicon using conventional methods for photonic application. *Superlattices Microstruct*. 52: 941–948.
[65] Martineau, F., K. Namur, J. Mallet, F. Delavoie, F. Endres, M. Troyon, and M. Molinari. 2009. Electrodeposition at room temperature of amorphous silicon and germanium nanowires in ionic liquid. *IOP Conf. Series: Materials Science and Engineering Symposium K, E-MRS 2009 Spring Meeting*. 012012.